This article has been accepted for publication in a future issue of this journal, but has not been fully edited. Content may change prior to final publication. Citation information: DOI 10.1109/JIOT.2020.3040713, IEEE Internet of Things Journal

Wireless Qi-powered, Multinodal and Multisensory Body Area Network for Mobile Health

Manik Dautta, Abel Jimenez, Kazi Khurshidi Haque Dia, *Member, IEEE,* Nafiul Rashid, *Member, IEEE,* Mohammad Abdullah Al Faruque, *Senior Member, IEEE,* and Peter Tseng

***Abstract*—Wireless, battery-free Body Area Networks (BAN) enable reliable long-term health monitoring with minimal intervention, and have the potential to transform patient care via mobile health monitoring. Current approaches for achieving such battery-free networks are limited in the number, capability, and positioning of sensing nodes–this is related to constraints in power supply, data rate, and working distance requirements between the wireless power source and sensing nodes. Here, we investigate a Qi-based, near-field power transfer scheme that can effectively drive wireless, battery-free, multi-node and multi-sensor BAN over long distances. This consists of a single Qi power source (such as a cellphone), a detached/untethered Passive Intermediate Relay (PIR) (facilitates power transfer from a central Qi source to multiple nodes on the body), and finally individual/detached sensing nodes placed throughout the body. Alongside this power scheme we implement the star network topology of a Gazell protocol to enable the continuous connection of one host to many sensing nodes while minimizing data loss over long temporal periods. The high-power transmission capabilities of Qi enables wireless support for a multitude of sensors (up to 12), and sensing nodes (up to 6) with a single transmitter at long distances (60 cm) and a sample rate of 20 Hz. This scheme is studied both in-vitro and in-vivo on the body.**

***Index Terms*—body area network, healthcare monitoring, wireless power transfer, wearable sensing, Gazell communication**

I. Introduction

SPATIALLY-DISTRIBUTED co-monitoring of physiological signals from various anatomical locations via Body Area Network (BAN) has the potential to enhance our understanding of the body and transform remote healthcare [1]–[3]. Recent studies have demonstrated the utility of wireless, battery-free sensors to measure a variety of biometric data, including temperature [4], [5], pressure [6], [7], bioelectric signals [8]–[10], heart rate [11], [12], pH [13], [14], strain [15]–[17], and more. Such sensors have found tremendous utility in health, ranging from enhancing our understanding of adult physiology [18]–[23], to monitoring vital signs during intensive neonatal care [24]–[26].

Wirelessly-powered wearable devices are rapidly emerging as an alternative to traditional battery-powered devices as they can be engineered to consume lower power, possess smaller size, promises to enhance user mobility, and reduce the need for user intervention [11], [27]–[29]. The immense flexibility in mobile healthcare by enabling continuous monitoring of multiple physiological parameters outside of the clinic or lab comes from the Wireless Power Transfer (WPT) and the remote operation of the systems [11], [15], [30], [31]. In general, typical battery-free systems utilize inductive powering and are most often based around near-field electromagnetic induction. Near-Field Communication (NFC) protocols require close (centimeter) proximity between the NFC reader and the NFC tag, and in such schemes, the reader only powers a single tag. This is tremendously limiting, as the reader must always have local access to the tag, meaning the tag must be exposed to the air and possess enough nearby air space to be accessible even for larger readers. Additionally, such approaches remain hampered due to low data rate, and sensitivity with respect to the relative position of transmitter and receiver.

The rest of this paper is organized as follows: Section II presents a brief discussion on related work, Section III presents the contributions of this paper, Section IV describes the experimental setup for the system design, characterization, and for real time data collection, Section V includes the discussion on obtained results, and Section VI draws conclusions of the works presented in this paper.

II. Related Work

Several strategies have been suggested to overcome the limitations associated with the NFC based powering and data transfer. One option is to simply add a power supply to the sensing tag/node so that it is no longer battery-free [32]–[35]. Batteries, however, come with many potential drawbacks–batteries are made from toxic materials and can potentially degrade and/or explode, batteries add significant weight to a device, and most importantly batteries do not last forever and must be changed depending on the power needs of the device. In keeping with the battery-free constraints, one approach is using a single, extremely large inductive coil to improve the distance and potentially power multiple tags [36], however, this approach is exceptionally power-hungry (and inefficient) as large volumes must be irradiated that are ultimately not utilized by the sensing tag/node. Another strategy is to embed multiple, cumbersome NFC readers directly into nearby structures (such as bedding) [25], [37]. This approach assumes that the sensing node/tag is static–this is not always the case–and additionally, such dispersed readers are effectively creating all-new nodes that will require independent powering. Intermediate relays have additionally been recently developed

All the authors are with the Department of Electrical Engineering and Computer Science, University of California Irvine, Irvine, CA, USA - 92697.

Peter Tseng is also with the Department of Biomedical Engineering, University of California Irvine, Irvine, CA, USA - 92697.

Email: {mdautta, abelj1, kdia, nafiulr, alfaruqu, tsengpc}@uci.edu.

Copyright (c) 20xx IEEE. Personal use of this material is permitted. However, permission to use this material for any other purposes must be obtained from the IEEE by sending a request to pubs-permissions@ieee.org.

2327-4662 (c) 2020 IEEE. Personal use is permitted, but republication/redistribution requires IEEE permission. See http://www.ieee.org/publications_standards/publications/rights/index.html for more information.
Authorized licensed use limited to: Access paid by The UC Irvine Libraries. Downloaded on January 27,2021 at 01:00:16 UTC from IEEE Xplore. Restrictions apply.

This article has been accepted for publication in a future issue of this journal, but has not been fully edited. Content may change prior to final publication. Citation information: DOI 10.1109/JIOT.2020.3040713, IEEE Internet of Things Journal

as a new technique to power battery-free sensors. A recently developed scheme utilizes a single NFC reader to wirelessly power multiple sensing nodes via an intermediate relay [38], however, this approach was limited to fairly moderate sample rates (1.3 Hz) when powering 6 nodes possessing a single sensor, and has a maximum of 8 Hz when powering a single sensor at a single node. This required a unique standalone NFC reader that possessed larger power transfer capabilities than typical NFC readers and is not available to most people. Such data rate limitations curb the accuracy of data coming from wearable sensors that require higher sampling rates, such as electrocardiography or accelerometers (20 Hz or higher).

In this paper, we developed a platform using the Qi technology that is uniquely able to resolve many of these issues. Qi can safely drive significantly more power vs. NFC standards (up to 30 W vs. 500 mW), and the Passive Intermediate Relay (PIR) is untethered and electrically insulated from all other components enabling significant RF power to drive a large network of sensors at high sample rates. As a proof of concept of the utility and scalability of this concept, we implemented a large set of sensors placed on a variety of nodes along the trunk and/or extremities of the body. These were utilized to continuously measure the complex, multi-sensory behavior of various points on the body during a variety of daily actions (gait, oral activity, exercise)–this is the core goal of BAN that seeks to better understand bodily behavior for many downstream applications related to health. This modular, versatile support of a large variety of sensors and nodes, all while utilizing easy-to-use battery-free sensors can be tuned to meet a variety of needs in healthcare monitoring.

III. Contributions of This Paper

The novel contributions of this paper are:

- We report a wireless, single Qi transmitter-powered, body area network capable of establishing wireless power and data connectivity between multiple, distant sensing nodes (each of which may consist of multiple sensors) around the body to create a wearable network of battery-free sensors. Our designed system is compatible with the tunable addition of sensing nodes and/or additional sensors with minimal further modification. Sensing nodes can be powered at 120cm distance from the sole Qi-transmitter with ~20% efficiency, and six sensing nodes at a 60cm distance from the transmitter with ~18% total efficiency.
- Qi interface standard devices operate around 200 kHz and typically transmit a dynamic medium power of up to 30 W (and will eventually support 200 W, Wireless Power Consortium - WPC). This is significantly higher than power delivered from the NFC standard (~500 mW). By utilizing the Qi standard, robust, multiple-sensor, multi-node body area networks can now be powered with single, commonly available Qi transmitters. Such medium power Qi transmitters radiate far lower Specific Absorption Rate (SAR) 0.08W/kg considered harmful for the human body [39], [40]. Qi is built into all modern cellphones, while most cellphones are unable to replicate the capabilities of stand-alone NFC readers required for higher-power, complex multi-node measurement. In addition, commercial Qi chargers are available powered from a variety of sources, including solar, battery-power packs, USB, and outlets.
- Passive Intermediate Relays (PIR) tuned to Qi standards are utilized to route RF power across long distances on the body, and overcome traditional limitations in near-field technology by powering sensing nodes far away from the transmitter. This intermediate relay is composed exclusively of conductive lanes, tuning capacitors, and transmitting inductors (passive RLC components). In addition, this component is completely detached/untethered and electrically-isolated from all other components of the system. Such a scheme is optimal for dynamic environments such as the body, which are in constant movement. Direct DC powering of nodes across the body would require exposed electrodes (a potential hazard), and whose rigid interconnections could readily be broken (either temporarily or permanently due to damage) during activity. These rigid restrictions become worse as more sensing nodes are added. The PIR method additionally gives better flexibility in terms of removing or modifying the network without worrying about interconnections. Such a component can be built into textiles or as an epidermal component.
- To overcome the bandwidth limitation in NFC technology, we utilize the Gazell protocol [41] for multinodal data communication. It possesses a star network topology and allows one host to connect with a multitude of devices, has bidirectional data transfer capability, enables packet acknowledgment and automatic packet retransmission, and is self-synchronizing to the host. In addition, the high-power transmission capabilities of Qi and versatility of the Gazell protocol enable the scalable addition of high-sample rate sensors and sensing nodes without concerns about the limitations in power and sample rate of NFC transmission. We have demonstrated a battery-free sensor network containing a multitude of sensors (12 demonstrated), and sensing nodes (up to 6) with a single transmitter at long distances (60 cm) at high sample rates (20 Hz), this significantly exceeds the existing NFC standard. It additionally allows up to 128 digital I2C sensors to be connected under the same network. Sensor data is continuously transmitted to a base station/cellphone for remote analysis.
- We demonstrate the compatibility of our system with the continuous monitoring of a wide variety of sensors (acoustic, pressure, strain, acceleration, temperature, bioelectric) placed on sensing nodes across the body, ranging from the arm, the trunk, to the legs. Our network is studied in-vivo for remote/mobile health monitoring in different scenarios such as gait/daily activities, oral activities, exercise/fitness tracking, all utilizing asymmetric sensing nodes (each sensing node consisting of different types of sensors as desired by the user). These demonstrations validate the utility of our approach to address emerging needs in mobile health, due to the scalability of Qi power, PIR, and Gazell protocols.

2327-4662 (c) 2020 IEEE. Personal use is permitted, but republication/redistribution requires IEEE permission. See http://www.ieee.org/publications_standards/publications/rights/index.html for more information.
Authorized licensed use limited to: Access paid by The UC Irvine Libraries. Downloaded on January 27,2021 at 01:00:16 UTC from IEEE Xplore. Restrictions apply.

This article has been accepted for publication in a future issue of this journal, but has not been fully edited. Content may change prior to final publication. Citation information: DOI 10.1109/JIOT.2020.3040713, IEEE Internet of Things Journal

IV. Experimental Setup

A. WPT System Design

The resonant inductive magnetic coupling based WPT system (Fig. 1) is composed of three detached components: transmitter, passive intermediate relay (PIR) and receiver (powering the sensing systems).

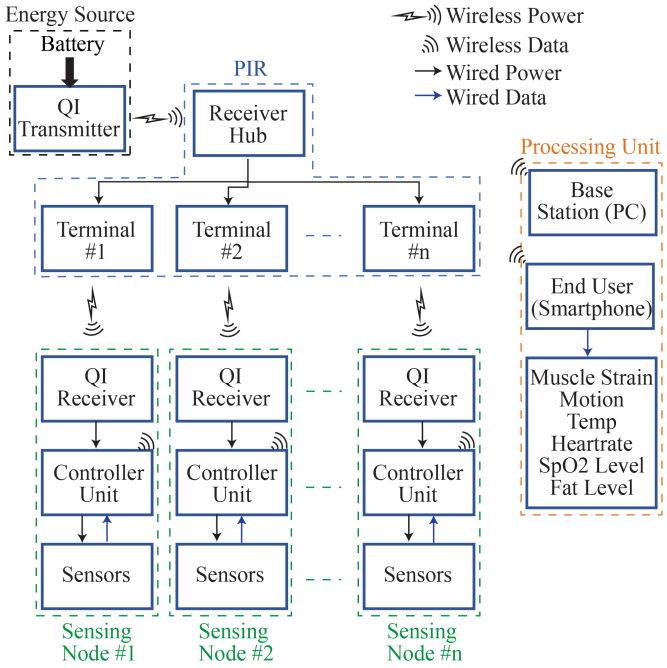

Fig. 1. Integration of the System.

The transmitter is a Qi wireless charging module based on an XKT-510 IC, which provides power to the network. The transmitter coil is 43mm diameter containing a 3.7μH inductance, and is capable of transmitting power at a maximum of 5W at 142kHz. 5V DC powers the micro controller inside the chip, and a TCXO generates the correct frequency of the AC signal that is then amplified by a full bridge MOSFET driver.

The PIR is composed of a 43mm diameter circular inductive coil of 14μH, together with a 100$\pm$10%nF tuning capacitor (of resonance frequency 142kHz) working as a receiver hub. This connects via long distance to multiple 43mm diameter circular inductive coils of 3.7μH working as terminals to provide wireless RF power to Qi receiver connected to sensor nodes.

Embedded systems at the sensing nodes contain a receiver in addition to sensors/microcontroller. This is the other part of the Qi wireless charging module, which has a 14μH 43mm diameter coil. The receiver is tuned by a capacitor of 100$\pm$10%nF to resonate at 142kHz to maximize the power transfer. The AC voltage is rectified to DC and regulated to 5V, which is synchronously controlled so that the micro controller inside the Qi receiver can turn on and off the transmitter to save power when not in use.

As a energy resource, we have restricted a 1W battery power to the Qi transmitter considering the safety issue which can come from the high current flow or the electromagnetic (EMF) radiation. In addition, there are now many different types of Qi charger options, ranging in power source (solar, battery/power bank, or outlet), to power supply capabilities (high power Qi can supply 15 kW!). These can be utilized for long term powering of BAN as required by the user if the cellphone is not sufficient.

B. Measurements and Simulation of RF Voltage

A 20cm single terminal PIR is used, while the vertical distances h_1, and h_2 are kept constant at 2mm. 1Vpp AC voltage of 142kHz is generated by a function generator (Keysight, 33220A) and applied to the port of the transmitter coil, and voltage is monitored at receiver hub, terminal and the receiver coil ports by a digital oscilloscope (Rigol, DS1054Z-B). To mimic the system, simulation is performed using PSpice/OrCAD. 1Vpp AC voltage of 142kHz signal is used as an input for the system, and two coupled inductors (coefficient of 0.5 and 0.8) are used to represent the transmitter-receiver hub and terminal-receiver coil.

C. WPT Efficiency Measurement

To measure the WPT efficiency, a 100Ω resistive load is added to the output of the receiver, and the PIR length d, vertical distances h_1, and h_2 are varied. Voltage drop and current flow are measured by a digital multimeter, and η is calculated using equation 1.

$$\eta = \frac{P_{out}}{P_{in}} 100\% = \frac{V_L I_L}{V_S I_S} 100\% \quad (1)$$

For simultaneous power transfer to multiple terminals, a 100Ω resistive load is added to each of six receiver outputs while keeping d constant at 60cm, and h_1=h_2=2mm. The overall η is calculated while varying the number of the terminal using equation 2.

$$\eta = \frac{P_{out}}{P_{in}} 100\% = \frac{\sum_i V_{L_i} I_{L_i}}{V_S I_S} 100\% \quad (2)$$

Here, V_S and I_S are the supply voltages (kept constant at 5V DC) and current to the transmitter, and V_L and I_L are the voltage and current in the 100Ω load.

D. Controller and Sensors at the Sensing Node

Sensors used in the experiments are: 3-axis accelerometer (ADXL345, Analog Device), piezoelectric sensor (LDTM-028K, TE Connectivity and AW-PAT41L, Audiowell Electronics), strain sensor (Flex Sensor, SpectraSymbol), acoustic sensor (Octopus Analog Noise Sound Sensor, Pi Supply), electromyography (EMG) sensor (Gravity Analog EMG Sensor, DFRobot), photoplethysmogram (PPG) sensor (Pulse Sensor Amped, Adafruit), and temperature sensor (NCP18WF104F03RC, Seeed Technology, and DS18B20, Maxim Integrated). All the sensors used in the experiment are noninvasive, and breakout boards are purchased off the shelf, while possessing a safe current limit for bio-applications. Microcontrollers used in the experiment are: RF-Duino (RFD22102) which possess a nRF51822 chip (Nordic

2327-4662 (c) 2020 IEEE. Personal use is permitted, but republication/redistribution requires IEEE permission. See http://www.ieee.org/publications_standards/publications/rights/index.html for more information.
Authorized licensed use limited to: Access paid by The UC Irvine Libraries. Downloaded on January 27,2021 at 01:00:16 UTC from IEEE Xplore. Restrictions apply.

This article has been accepted for publication in a future issue of this journal, but has not been fully edited. Content may change prior to final publication. Citation information: DOI 10.1109/JIOT.2020.3040713, IEEE Internet of Things Journal

Semiconductor, an ARM Cortex M0 microcontroller, Flash and RAM memory, the BLE chipset), and circuit playground classic (Adafruit, ATmega32u4 processor).

Specific sensors utilized at the respective nodes of our BAN are listed in TABLE I.

TABLE I
SENSING NODES USED IN OUR BAN

Node No.	Node Position	Sensor Name
1	Left Wrist	One 3-axis Accelerometer
2	Throat	One Piezoelectric, One Strain, One Acoustic
3	Right Chest	One ECG, One Temperature
4	Right Elbow	One Strain, One EMG
5	Right Wrist	One Strain, One PPG
6	Right Knee	One 3-axis Accelerometer
7	Left Ankle	One 3-axis Accelerometer

E. In-Vitro RF Power Transfer and Communication Demonstration

5V DC is applied to the transmitter and h_1=h_2 are kept constant at 3mm. To demonstrate Qi's potential to supply significant power to a single node, a 100cm single terminal PIR is used to power an Adafruit Circuit Playground containing 12 LEDs in total. Two LEDs, one small green and small red LED, show when the board achieves power connection and switches on a pathway that serially activates 10 LEDs. To demonstrate Qi's potential to supply power to multiple nodes, a six terminal PIR (60cm length) is used to power six nodes. These nodes either have one LED, or one sensing node consists of one RFDuino module, one piezoelectric sensor and one temperature sensor. Simultaneous sensor data from all nodes are transferred at 20Hz to the base station (another RFDuino connected to a computer).

F. Real Time Data Collection from the Wireless Sensing Nodes

While ECG/EMG electrodes, strain, and piezoelectric sensors are placed directly on the skin, all other sensors, control circuitry, and Qi receiver are isolated inside a 3D printed box. The receiver coil of the sensing node is placed at the bottom of the box. The PIR, designed to provide RF power between physically separated Qi transmitter and a baterry-free sensor network, is embossed on a vinyl and attached to the skin by a double-sided tape–this completely isolates the PIR to prevent any accidental electrical shock or any discomfort due to the generated heat. Data is collected wirelessly by Gazell protocol at 20Hz sampling frequency. EMF radiation above 1mG is considered to be harmful to the human body, and medium Qi power is rated to be used near humans and radiates below this limit (and enables its utilization in cellphones and chargers). Our currently demonstrated BAN, however, possesses fairly low power requirements and was readily powered by a Qi Tx restricted to 1 W. However, this can readily scale to various applications and needs.

1) Continuous Wireless Exercise Monitoring: Data for continuous wireless exercise measurements are collected from the sensing node 1, where a 3-axis accelerometer is placed on the left wrist. The PIR embossed on the vinyl substrate is placed on the arm, while the receiver hub is on the elbow and the terminal is under the receiver coil on the wrist. A healthy human subject is instructed to rest by standing up straight while keeping the hand at the side, to do front raising and subsequently triceps pulldown.

2) Continuous Wireless Gait/Multinodal Daily Activity Monitoring: Data for continuous wireless gait measurements are collected from sensing node 7 (left ankle), and for daily activity monitoring simultaneously from sensing node 6 (right knee) and sensing node 7. The terminal part of the relay is placed under the receiver coil of the sensing node, and the receiver hub part is placed on the back-pocket where it gets power from the transmitter. A healthy human subject is instructed to rest by sitting on a chair, walk on a plain surface, and then run slowly for gait monitoring. Afterwards, the subject is asked to walk upstairs, walk on a plain surface, and then walk downstairs for multinodal daily activity monitoring.

3) Multisensor Oral Activity Monitoring: Data for multisensor oral activity monitoring are collected from sensing node 2 placed on the throat by a neckband, where the piezoelectric sensor is placed on the Adam's apple, the acoustic sensor is placed on the vocal cord, and the strain sensor is placed on the jaw. The terminal part of the PIR is placed on the throat and the receiver hub is placed under the left chest pocket area, in order to receive power from the transmitter placed in the pocket. A healthy human subject is instructed to read, to be idle/silent and to chew a gum.

4) Multinodal Multisensory Fitness Tracking: Data for multinodal multisensory fitness tracking is collected simultaneously form sensing node 3 (ECG and temperature sensor - right chest), sensing node 4 (strain sensor-elbow, EMG sensor -shoulder), and sensing node 5 (a PPG and a strain sensor placed on the finger and arm respectively). The three terminal parts of the PIR are placed under the respective sensing nodes, and the receiver hub is placed under the left chest pocket area where it aligns with the Qi transmitter. A healthy human subject is instructed to rest, do pushup, and do dip exercises.

V. RESULTS AND DISCUSSION

A. System Design and Characterization

When a wireless Qi power transmitter [42] is placed in close proximity to the receiver hub side of the PIR, a time-varying magnetic field of signal frequency 142kHz induces current throughout the relay. This generates magnetic fields simultaneously at terminal ends of the relay, thus enabling wireless powering of a baterry-free sensor network that are beyond the standard range of the transmitter (Fig. 2a). Each sensing node of the network receives power independently, and collects data from different places on the body (Table I). These nodes transmit signals wirelessly to the base/user station via Gazell protocol for remote analysis.

Fig. 2b shows the methodology of PIR, which consists of a central receiver hub and an output terminal where the central receiver hub is a loop antenna with a tuning capacitor connected to an output terminal via enamel wire. The central receiver hub receives RF power from a Qi wireless power transmitter and sends the current to the connected output

2327-4662 (c) 2020 IEEE. Personal use is permitted, but republication/redistribution requires IEEE permission. See http://www.ieee.org/publications_standards/publications/rights/index.html for more information.
Authorized licensed use limited to: Access paid by The UC Irvine Libraries. Downloaded on January 27,2021 at 01:00:16 UTC from IEEE Xplore. Restrictions apply.

This article has been accepted for publication in a future issue of this journal, but has not been fully edited. Content may change prior to final publication. Citation information: DOI 10.1109/JIOT.2020.3040713, IEEE Internet of Things Journal

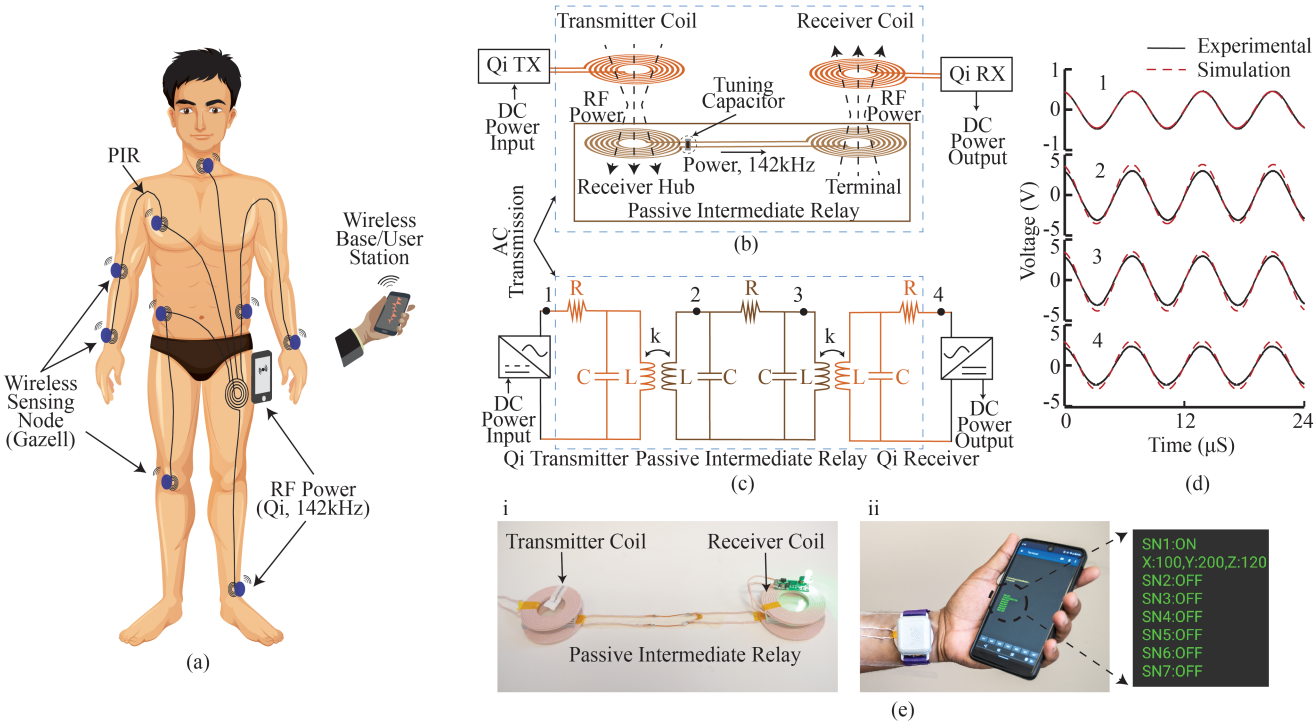

Fig. 2. Qi-powered, multinodal multisensory BAN for healthcare monitoring. a) Schematic of BAN (human figure is modified from Vecteezy), b) Schematic diagram of the WPT, c) Simplified circuit diagram, d) Voltage at points 1 to 4 in c. e) Wireless activation of an LED (i), Data transmission to the wireless base/user station (ii).

terminal. The output terminal then acts as a wireless power transmitter and powers a sensing node's receiver coil. Such relays overcome the major limitation of near field power transfer technology, which functions only within the close proximity of the reader (for example, the Qi charging transmitter/receiver pair can only be separated by 2-10mm) [43], [44]. This extra range can provide wireless power to battery-free sensor networks. The configuration can be modelled by a simplified circuit shown in Fig. 2c, where the intermediate relay is a passive LC resonator tuned to operate at Qi operation frequency. Qi transmitter converts the DC to AC and transfers the RF power through the PIR. After receiving the RF power from the terminal, the receiver converts the AC to DC to power the sensing nodes consisted of a microcontroller, BLE antenna and sensors. Fig. 2d shows voltage at different points of the system (20cm PIR length) monitored by a digital oscilloscope when 1Vpp AC is applied by a function generator at point 1. PSpice/OrCAD simulation results show close agreement with the experimental results. Due to the resonance of the system, voltage at the receiver hub end (point 2) is amplified by almost 6 times. After transmission of 20cm, voltage remains at the same level at the terminal end (point 3), which indicates the low loss AC transmission in a resonance system (at resonance there is no reactive loss in AC system). The highly efficient power transfer capability between the PIR terminal and end Qi receiver retains the voltage at almost the same level at the receiver coil end (point 4). This illustrates the efficient power transfer of Qi transmitter/receiver between two physically separated locations over long distance.

Fig. 2e demonstrates the functionality of the power transfer and the data communication in a mobile health system. With the vertical distances h_1 and h_2 set to 5mm, a 5V DC supply at the transmitter results in activation of a LED connected at the output of the receiver module separated by 20cm from the transmitter (Fig. 2e-i). Similarly, Fig. 2e-ii shows the positional data wirelessly transferred from a sensing node 1 consists of a 3-axis accelerometer placed on the left wrist to the smartphone while other sensing nodes are in OFF state.

1) WPT Efficiency Characterization : We first evaluate the WPT efficiency (η) of a single Qi Tx/Rx without PIR (Fig. 3a-i). Fig. 3a-ii and 3a-iii show η decreases rapidly without PIR with the vertical distance h and horizontal distance d between the transmitter and the receiver/sensing node. This happens because when properly terminated, the magnetic field stays between the transmitter and the receiver coil, and the field decreases rapidly with the vertical/horizontal separation between them. This approach offers maximum reliable operation up to a few millimeters.

Then we measure η of a single Qi Tx/Rx with a PIR. We first measure η of the system of a 20cm single terminal PIR, by varying the distance h_1 while keeping the terminal and receiver coils in close contact (h_2=0 means the coils are separated only by the insulating material of the conductors). Fig. 3b-ii shows the maximum η (23%) occurs at h_1=4mm while it drops at below 4mm due to over-coupling and above 4mm due to under-coupling between the transmitter and receiver hub coil. Then we measure η of the same system by varying the distance h_2, while keeping h_1 at 5mm. Fig. 3b-iii shows η

2327-4662 (c) 2020 IEEE. Personal use is permitted, but republication/redistribution requires IEEE permission. See http://www.ieee.org/publications_standards/publications/rights/index.html for more information.
Authorized licensed use limited to: Access paid by The UC Irvine Libraries. Downloaded on January 27,2021 at 01:00:16 UTC from IEEE Xplore. Restrictions apply.

This article has been accepted for publication in a future issue of this journal, but has not been fully edited. Content may change prior to final publication. Citation information: DOI 10.1109/JIOT.2020.3040713, IEEE Internet of Things Journal

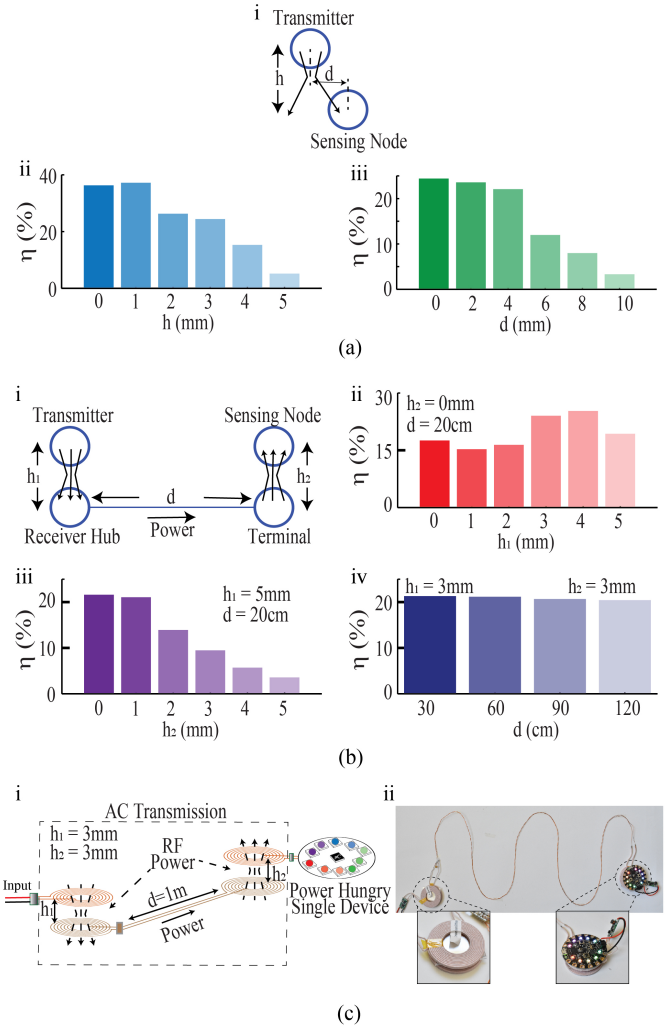

Fig. 3. WPT Efficiency (η) of a Single Qi One Node System. a) Schematic diagram (i), η measurement by varying the distance h (ii), and d (iii) without PIR, b) Schematic diagram (i), η measurement by varying the distance h_1 (ii), h_2 (iii), and d (iv) with PIR, c) Schematic diagram (i), and power transfer to a Circuit Playground (ii) with PIR.

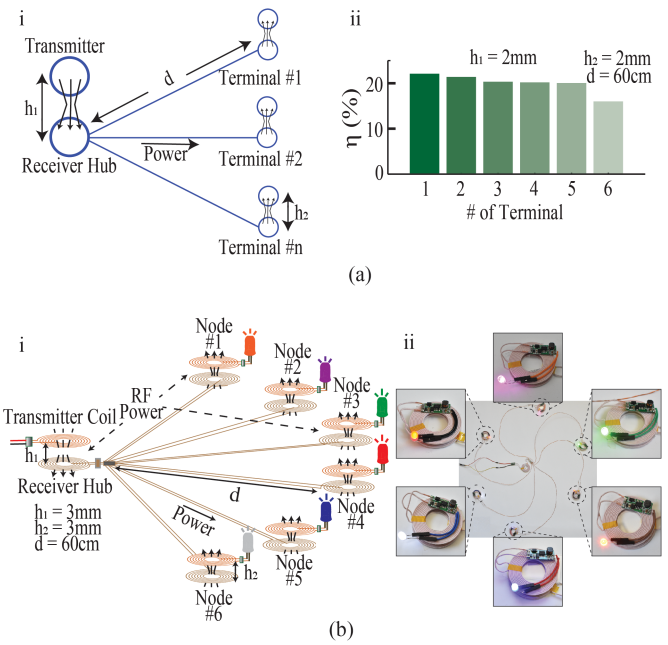

Fig. 4. WPT Efficiency (η) of a Multinode system. a) Schematic diagram (i), η measurement by varying the number of terminals (ii). b) Schematic diagram (i), and power transfer to six LED nodes (ii).

drops while increasing the h_2 due to under-coupling between the terminal and the receiver coils. Then we investigate η of the system by varying the PIR length d while keeping h_1 and h_2 constant at 3mm. Initially η without the PIR is little higher than with PIR when the h_2 is varying in Fig. 3b-iii, however decreases rapidly compared to varying h_1 in Fig. 3b-ii. As the system is operating at resonance, the only loss of the system is the parasitic loss as d increases. The η at d=30cm is 21.3%, which decreases to 20.4% at d=120cm (Fig. 3b-iv). This confirms the peaks of radiation in the PIR are located directly adjacent to the inductor nodes terminated by the receiver and not elsewhere in the PIR. To validate the high power delivered by Qi and our PIR to a single sensing node over a long distance, experimental demonstration is done by powering a Circuit Playground Classic of having 10 LEDs over 100cm distance using a single terminal PIR (Fig. 3b).

Then we study the efficiency of simultaneous Qi power transfer to multiple receivers using a multi-terminal single receiver hub PIR. The PIR facilitates the efficient transfer of RF power from a single central Qi transmitter to the sensor network (i.e., multiple sensing nodes) which removes the requirement of multiple energy sources to power each of the individual sensing nodes. In DC, each sensor node must be connected directly via an interconnect to the power supply. In the case of interconnect failure at a single node, exposed electrodes can be flanking the body, potentially becoming hazardous as the power supply tries to power the remaining sensing nodes. No such hazard exists with the PIR as it is completely untethered and electrically isolated, and if a sensing node becomes misaligned, the rest of the sensing nodes can continue to operate without issue to the user. Unlike a fixed power output transmitter, where the transfer efficiency is inversely proportional to the number of terminals, the dynamic high-power Qi transmitter is capable of supplying required power when the load increases at the sensing nodes, given that the system is tuned to operate at resonance and the battery is capable of supplying enough current. We investigate η by increasing the number of the terminals, which is 22% for a single terminal and 17% for six terminals for d= 60cm, h_1=h_2=2mm (Fig. 4a-ii). The η drops slightly because of minor off-tuning, as well as current limitations of the battery used as the energy resource to reduce accidental excess current. To validate the power delivered at the multiple sensing nodes over a long distance, experimental demonstration is done similar to as in Fig. 3b, by powering up six terminals over 60cm distance connected in parallel to the single receiver hub. Powering the transmitter results in robust activation of six LEDs connected to six receivers while keeping the h_1=h_2=3mm (Fig. 4b).

2) Demonstration of Wireless Communication : Operating multiple sensors generally requires more power, while at the same time reduces the maximum data rate for the entire

2327-4662 (c) 2020 IEEE. Personal use is permitted, but republication/redistribution requires IEEE permission. See http://www.ieee.org/publications_standards/publications/rights/index.html for more information.
Authorized licensed use limited to: Access paid by The UC Irvine Libraries. Downloaded on January 27,2021 at 01:00:16 UTC from IEEE Xplore. Restrictions apply.

This article has been accepted for publication in a future issue of this journal, but has not been fully edited. Content may change prior to final publication. Citation information: DOI 10.1109/JIOT.2020.3040713, IEEE Internet of Things Journal

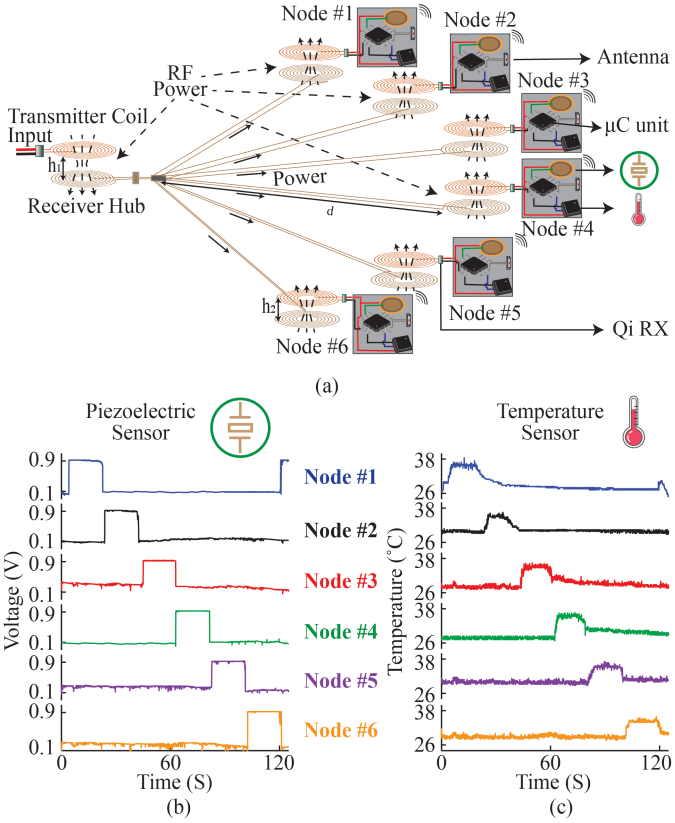

Fig. 5. Continuous Wireless Communication of Multinodal Multisensory System. a) Schematic diagram, b) Piezoelectric sensors data, c) Temperature sensors data.

system. However, here a star topology Gazell protocol is used to establish a high data rate communication link. It supports bidirectional data transfer allowing control of the devices, and enabling their deactivation when not in use to save power. Gazell has packet acknowledgement and automatic packet re-transmission allowing guaranteed data quality. Supplementary Fig. S1 shows the major steps in communication between sensing nodes and base station, as well as the data transfer mechanism.

To validate the multinodal multisensory data transfer, in-vitro experimental measurements are done by using a 60 cm PIR of having a single receiver hub connected to six terminals in parallel. Each node consisted of a RFDuino module (a microcontroller and an antenna), a touch sensitive piezoelectric sensor and a temperature sensor connected to a Qi receiver module shown schematically in Fig. 5a, while the experimental setup is shown in Supplementary Fig. S2. Pressing the touch sensor increases the capacitance of the piezoelectric sensor (which in turn increases the voltage output, Fig. 5b), while flowing hot air into the temperature sensor increases resistance of the thermistor (which results in more voltage drops across it Fig. 5c). Each of the six nodes consisted of two sensors, comprising in total 12 sensors transmitting data to the base station at 20Hz simultaneously in real time. This demonstrates the capability of Qi to robustly power numerous nodes and sensors in real-time using this technique.

B. Continuous Wireless Exercise Monitoring

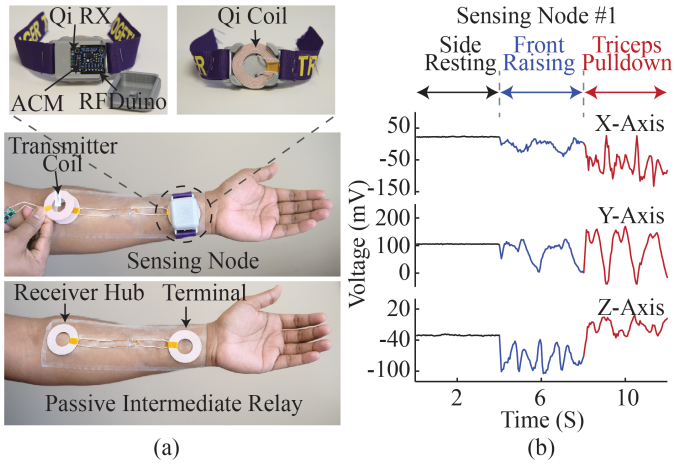

Fig. 6. Continuous Wireless Exercise Monitoring. a) Placement of the transmitter, PIR, and sensing node, b) xyz-axis motion measurements data.

Continuous operation of devices during exercise requires optimal placement of sensors, stable power input, and secure connectivity to the central processing unit. Biosensors are often powered either by battery (which can give stable output power but possess hazardous chemical/electrical threat to body), or via near-field power supplied directly at the sensing node (requiring close proximity to the transmitter). This is overcome by the RF power transmitting PIR, which transmits power from the transmitter to the sensing node placed in mutiple locations. We first test a basic two position/node monitoring system for real-time exercise monitoring. This includes a motion sensing node on the wrist (Fig. 6), and gait measurement by placing a motion sensing node on the left ankle (Supplementary Fig. S3).

Fig. 6a shows an example of the placement of the PIR, transmitter and the sensing node. The sensing node consisted of a RFDuino controller unit, a 3-axis accelerometer connected to the Qi receiver module placed inside of the box, while the receiver coil is placed outside of the box. Fig. 6b shows motion measurements data which are acquired from the battery-free sensing node 1, during the resting (hands are in side), front raising, and triceps pulldown phases while the PIR is placed on the arm (this was embossed on vinyl to enable conformation to the skin). While there is no acceleration in any axis during the resting phase, there are large accelerations in the y and z axis during front raising, and in the x and y axis during triceps pulldown phase. Basic signal processing can be applied in the fog or cloud to track/differentiate activity by extracting the features such as peak amplitude, peak to peak interval, peak duration, peak shape. Data is acquired in real-time at a 20Hz sampling rate without any loss of connectivity over the 15-min duration of the protocol. Such mobile health monitoring methods can be used for detecting many potential health risks such as ER/UR care for physically disabled people, for neurodegenerative disorders, reduced motor function of diabetic subjects, rehabilitation from as physical therapy, and as well as training for athletic/military personnel.

2327-4662 (c) 2020 IEEE. Personal use is permitted, but republication/redistribution requires IEEE permission. See http://www.ieee.org/publications_standards/publications/rights/index.html for more information.
Authorized licensed use limited to: Access paid by The UC Irvine Libraries. Downloaded on January 27,2021 at 01:00:16 UTC from IEEE Xplore. Restrictions apply.

This article has been accepted for publication in a future issue of this journal, but has not been fully edited. Content may change prior to final publication. Citation information: DOI 10.1109/JIOT.2020.3040713, IEEE Internet of Things Journal

C. Multinodal Activity Monitoring

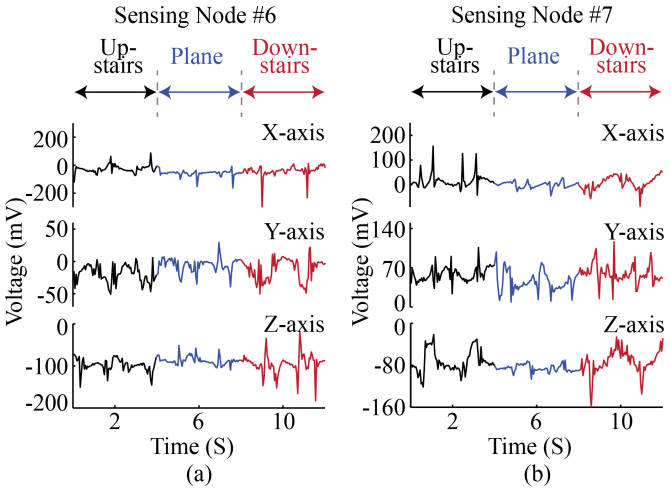

Fig. 7. Continuous Multinodal Daily Activity Monitorig. 3-axis accelerometer data from a) sensing node 6, and b) sensing node 7.

BAN possess unique requirements due to the fact that the body is constantly in motion, often require a variety of sensors (placed on many nodes) operating at high sampling rate to properly capture information, and possess unique safety concerns (i.e. open electrodes passing current and/or batteries can become hazardous). The untethered and completely active electronics free PIR removes such hazards, and continues to operate the rest of the sensing nodes even when one of the them is misaligned or faulty. This approach is uniquely scalable and modular in comparison to existing concepts in BAN. In addition, While operating multiple sensors requires more power and at the same time it produces electromagnetic radiation which might be concerning for the user acceptance, the current Gazell protocol and sensors in this paper are readily powered by a Qi Tx restricted to 1 W which radiates far lower SAR than 0.08 W/kg above which is considered harmful for the human body.

Fig. 7a shows the representative signals collected from sensing node 6 placed on the right knee, Fig. 7b from sensing node 7 placed on left ankle both of which consists of a 3-axis accelerometer. Data is acquired from two different sensing nodes at 20Hz sampling rate simultaneously during walking upstairs, in a plane surface, and downstairs phases wirelessly when powered by a single Qi transmitter placed on the back pocket. Although a post signal processing is required to label the data relating to the activity monitoring like elderly fall detection, physical muscle therapy and more, data can be discriminating from normal daily activity monitoring by looking at pattern. Such as walking on the plain surface produces more acceleration in the y axis than x and z axis shown in the data from both nodes. On the other hand the sensor placed in the ankle had higher acceleration that the sensor placed in the knee.

D. Multinodal Multisensory Fitness Tracking

Multimodal, spatiotemporal physiological data collected from different locations on the body may help improve our understanding of anatomy, as well as assess potential health issues. Robust measurement requires the collection of data from multiple types of sensors placed at varying positions of the body. Such multinodal, multisensory measurement is currently limited when using battery-free BAN based around WPT. Current techniques utilizing NFC-based readers exhibit power and bandwidth limitations that prevent the aggressive scaling of sensor number and positions. Here we utilize the high WPT capabilities of Qi, in conjunction with one intermediate relay having one receiver hub but multiple terminals. This enables a single Qi power transmitter to wirelessly power multiple sensing nodes consisting of multiple sensors. The resulting monitoring system is utilized to enable real time oral activity monitoring (Supplementary Fig. S4), and exercise/fitness tracking (Fig. 8).

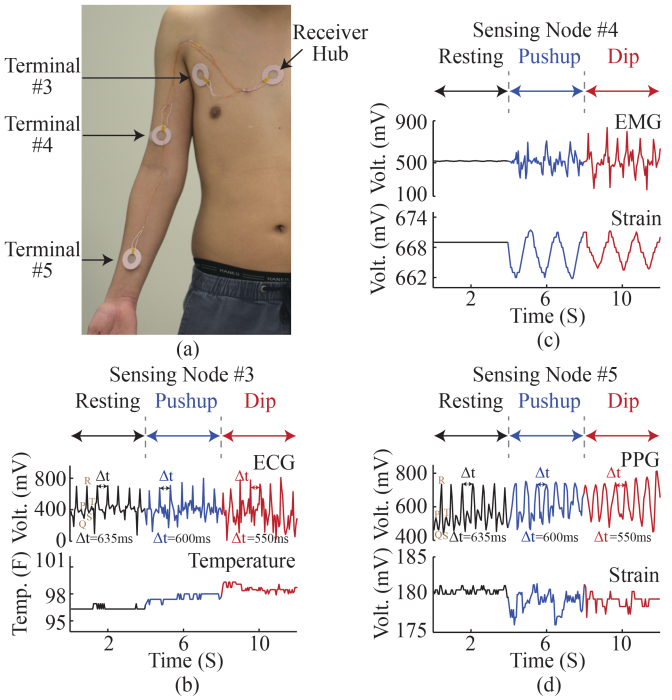

Fig. 8. Continuous Multinodal Multisensory Fitness Tracking. a) Placement of a three terminal PIR, b) ECG and Temperature sensor data from sensing node 3, c) EMG and Strain sensor data from sensing node 4, and d) PPG and Strain sensor data from sensing node 5.

Fig. 8a shows the placement of the Qi-based, PIR multinodal multisensory setup for fitness tracking. Fig. 8b shows the representative signals collected from sensing node 3 placed on the chest (ECG, Temperature), Fig. 8c from sensing node 4 placed on right elbow (EMG, Strain), and Fig. 8d from sensing node 5 placed on the right arm (PPG, Strain). Data is acquired from all three sensing nodes (total of six sensors, 20 Hz sample rate) simultaneously during the resting, push up, and dip exercise phases wirelessly when powered by a single Qi transmitter placed on the chest pocket. Heartrate is increased when switching from resting (95 bpm) to push-up (100 bpm) to dip (109 bpm) exercise phases. Temperature sensor shows that temperature is increased during both the push up and dip phase, but as the subject gets tired, temperature went down slowly due to the respiration effect. EMG signal shows

2327-4662 (c) 2020 IEEE. Personal use is permitted, but republication/redistribution requires IEEE permission. See http://www.ieee.org/publications_standards/publications/rights/index.html for more information.
Authorized licensed use limited to: Access paid by The UC Irvine Libraries. Downloaded on January 27,2021 at 01:00:16 UTC from IEEE Xplore. Restrictions apply.

This article has been accepted for publication in a future issue of this journal, but has not been fully edited. Content may change prior to final publication. Citation information: DOI 10.1109/JIOT.2020.3040713, IEEE Internet of Things Journal

the muscle stress on the shoulder, while the strain sensor placed on the shoulder captured the shoulder motion. The strain sensor placed on the wrist is unchanged, because during the push up and dip phase the subject was instructed not to move/stretch the arm. Such demonstrated spatiotemporal physiological signal collection (sampled at a robust 20 Hz) from different anatomical locations with multiple sensors can be used in a variety healthcare monitoring systems for point-of-care application in remote settings.

VI. Conclusion

Continuous physiological monitoring for mobile health using battery-free Body Area Networks is traditionally hampered by a limited number of sensing nodes, as well as the number and type of sensors at individual nodes. By utilizing Qi-driven wireless power in conjunction with recently investigated passive intermediate relays (PIR), we overcome a number of traditional limitations typically associated with wirelessly powered, battery-free body area networks. The extra power afforded by Qi allows multiple sensing nodes and multiple sensors to function off a single Qi power source. This is combined with a PIR to enable wireless support of a battery-free sensor network containing a multitude of sensors (12 demonstrated), and sensing nodes (up to 6) with a single transmitter at long distances (60 cm) at high sample rates (20 Hz). This PIR is not directly connected to the other components, and is completely electrically isolated from the body. This reduces safety issues that could crop up from DC powering of multiple sensing nodes, and could potentially be integrated into textiles or epidermal electronics. In addition, the high-power transmission capabilities of Qi and versatility of the Gazell protocol may enable the scalable addition of high-sample rate sensors and sensing nodes without concerns about the limitations in power and sample rate of NFC transmission. Qi is built into all modern cellphones which are inherently capable of BLE connectivity, while most cellphones are unable to replicate the capabilities of stand-alone NFC readers required for complex multinode measurement. We anticipate this approach to have a variety of applications within physiological tracking, while reducing reliance on batteries, enabling smaller sensor nodes, and facilitating long-term mobile health monitoring with minimal intervention.

Acknowledgment

This work was supported by faculty startup granted by the University of California Irvine (UCI), and was partially supported by the National Science Foundation through the CAREER award through ECCS-1942364, as well as the National Institutes of Health through R21CA239249. Experiments involving human subjects were performed with informed consent under protocol HS#2018-4843 from the UCI Institutional Review Board.

References

[1] R. A. Khan and A.-S. K. Pathan, "The state-of-the-art wireless body area sensor networks: A survey," *International Journal of Distributed Sensor Networks*, vol. 14, no. 4, p. 1550147718768994, 2018.

[2] A. Azim and M. M. Islam, "Hybrid leach: A relay node based low energy adaptive clustering hierarchy for wireless sensor networks," in *2009 IEEE 9th Malaysia International Conference on Communications (MICC)*. IEEE, 2009, pp. 911–916.

[3] M. S. Mahmud, H. Wang, A. Esfar-E-Alam, and H. Fang, "A wireless health monitoring system using mobile phone accessories," *IEEE Internet of Things Journal*, vol. 4, no. 6, pp. 2009–2018, 2017.

[4] Y. Jiang, K. Pan, T. Leng, and Z. Hu, "Smart textile integrated wireless powered near field communication (nfc) body temperature and sweat sensing system," *IEEE Journal of Electromagnetics, RF and Microwaves in Medicine and Biology*, 2019.

[5] S. R. Krishnan, C.-J. Su, Z. Xie, M. Patel, S. R. Madhvapathy, Y. Xu, J. Freudman, B. Ng, S. Y. Heo, H. Wang *et al.*, "Wireless, battery-free epidermal electronics for continuous, quantitative, multimodal thermal characterization of skin," *Small*, vol. 14, no. 47, p. 1803192, 2018.

[6] L. Y. Chen, B. C.-K. Tee, A. L. Chortos, G. Schwartz, V. Tse, D. J. Lipomi, H.-S. P. Wong, M. V. McConnell, and Z. Bao, "Continuous wireless pressure monitoring and mapping with ultra-small passive sensors for health monitoring and critical care," *Nature communications*, vol. 5, no. 1, pp. 1–10, 2014.

[7] P.-J. Chen, D. C. Rodger, S. Saati, M. S. Humayun, and Y.-C. Tai, "Microfabricated implantable parylene-based wireless passive intraocular pressure sensors," *Journal of Microelectromechanical Systems*, vol. 17, no. 6, pp. 1342–1351, 2008.

[8] W. Gao, S. Emaminejad, H. Y. Y. Nyein, S. Challa, K. Chen, A. Peck, H. M. Fahad, H. Ota, H. Shiraki, D. Kiriya *et al.*, "Fully integrated wearable sensor arrays for multiplexed in situ perspiration analysis," *Nature*, vol. 529, no. 7587, pp. 509–514, 2016.

[9] U. Varshney, "Pervasive healthcare and wireless health monitoring," *Mobile Networks and Applications*, vol. 12, no. 2-3, pp. 113–127, 2007.

[10] H. Kazemi, A. Hajiaghajani, M. Y. Nada, M. Dautta, M. Alshetaiwi, P. Tseng, and F. Capolino, "Ultra-sensitive radio frequency biosensor at an exceptional point of degeneracy induced by time modulation," *arXiv preprint arXiv:1909.03344*, 2019.

[11] W.-Y. Chung, Y.-D. Lee, and S.-J. Jung, "A wireless sensor network compatible wearable u-healthcare monitoring system using integrated ecg, accelerometer and spo 2," in *2008 30th Annual International Conference of the IEEE Engineering in Medicine and Biology Society*. IEEE, 2008, pp. 1529–1532.

[12] K. Arquilla, A. K. Webb, and A. P. Anderson, "Textile electrocardiogram (ecg) electrodes for wearable health monitoring," *Sensors*, vol. 20, no. 4, p. 1013, 2020.

[13] A. J. Bandodkar, P. Gutruf, J. Choi, K. Lee, Y. Sekine, J. T. Reeder, W. J. Jeang, A. J. Aranyosi, S. P. Lee, J. B. Model *et al.*, "Battery-free, skin-interfaced microfluidic/electronic systems for simultaneous electrochemical, colorimetric, and volumetric analysis of sweat," *Science advances*, vol. 5, no. 1, p. eaav3294, 2019.

[14] M. Dautta, M. Alshetaiwi, A. Escobar, F. Torres, N. Bernardo, and P. Tseng, "Multi-functional hydrogel-interlayer rf/nfc resonators as a versatile platform for passive and wireless biosensing," *Advanced Electronic Materials*, vol. 6, no. 4, p. 1901311, 2020.

[15] S. Niu, N. Matsuhisa, L. Beker, J. Li, S. Wang, J. Wang, Y. Jiang, X. Yan, Y. Yun, W. Burnett *et al.*, "A wireless body area sensor network based on stretchable passive tags," *Nature Electronics*, vol. 2, no. 8, pp. 361–368, 2019.

[16] S. Cheng and Z. Wu, "A microfluidic, reversibly stretchable, large-area wireless strain sensor," *Advanced functional materials*, vol. 21, no. 12, pp. 2282–2290, 2011.

[17] L. Lin, M. Dautta, A. Hajiaghajani, A. Escober, P. Tseng, and M. Khine, "Paint-on epidermal electronics for on-demand sensors and circuits," *Advanced Electronic Materials*, 2020, doi: 10.1002/aelm.202000765.

[18] A. Burton, T. Stuart, J. Ausra, and P. Gutruf, "Smartphone for monitoring basic vital signs: Miniaturized, near-field communication based devices for chronic recording of health," in *Smartphone Based Medical Diagnostics*. Elsevier, 2020, pp. 177–208.

[19] N. Anabtawi, S. Freeman, and R. Ferzli, "A fully implantable, nfc enabled, continuous interstitial glucose monitor," in *2016 IEEE-EMBS International Conference on Biomedical and Health Informatics (BHI)*. IEEE, 2016, pp. 612–615.

[20] W.-J. Yi and J. Saniie, "Smart mobile system for body sensor network," in *IEEE International Conference on Electro-Information Technology, EIT 2013*. IEEE, 2013, pp. 1–4.

[21] H. Jeong, L. Wang, T. Ha, R. Mitbander, X. Yang, Z. Dai, S. Qiao, L. Shen, N. Sun, and N. Lu, "Modular and reconfigurable wireless e-tattoos for personalized sensing," *Advanced Materials Technologies*, vol. 4, no. 8, p. 1900117, 2019.

2327-4662 (c) 2020 IEEE. Personal use is permitted, but republication/redistribution requires IEEE permission. See http://www.ieee.org/publications_standards/publications/rights/index.html for more information.
Authorized licensed use limited to: Access paid by The UC Irvine Libraries. Downloaded on January 27,2021 at 01:00:16 UTC from IEEE Xplore. Restrictions apply.

This article has been accepted for publication in a future issue of this journal, but has not been fully edited. Content may change prior to final publication. Citation information: DOI 10.1109/JIOT.2020.3040713, IEEE Internet of Things Journal

[22] N. Rashid, M. Dautta, P. Tseng, and M. A. Al Faruque, "Hear: Fog-enabled energy aware online human eating activity recognition," *IEEE Internet of Things Journal*, 2020, early Access doi: 10.1109/JIOT.2020.3008842.

[23] M. Dautta, M. Alshetaiwi, J. Escobar, and P. Tseng, "Passive and wireless, implantable glucose sensing with phenylboronic acid hydrogel-interlayer rf resonators," *Biosensors and Bioelectronics*, vol. 151, p. 112004, 2020.

[24] H. U. Chung, A. Y. Rwei, A. Hourlier-Fargette, S. Xu, K. Lee, E. C. Dunne, Z. Xie, C. Liu, A. Carlini, D. H. Kim *et al.*, "Skin-interfaced biosensors for advanced wireless physiological monitoring in neonatal and pediatric intensive-care units," *Nature Medicine*, vol. 26, no. 3, pp. 418–429, 2020.

[25] H. U. Chung, B. H. Kim, J. Y. Lee, J. Lee, Z. Xie, E. M. Ibler, K. Lee, A. Banks, J. Y. Jeong, J. Kim *et al.*, "Binodal, wireless epidermal electronic systems with in-sensor analytics for neonatal intensive care," *Science*, vol. 363, no. 6430, 2019.

[26] H. Chen, S. Bao, C. Lu, L. Wang, J. Ma, P. Wang, H. Lu, F. Shu, S. B. Oetomo, and W. Chen, "Design of an integrated wearable multisensor platform based on flexible materials for neonatal monitoring," *IEEE Access*, vol. 8, pp. 23 732–23 747, 2020.

[27] J. Kim, G. A. Salvatore, H. Araki, A. M. Chiarelli, Z. Xie, A. Banks, X. Sheng, Y. Liu, J. W. Lee, K.-I. Jang *et al.*, "Battery-free, stretchable optoelectronic systems for wireless optical characterization of the skin," *Science advances*, vol. 2, no. 8, p. e1600418, 2016.

[28] A. H. A. Zargari, M. Dautta, M. Ashrafiamiri, M. Seo, P. Tseng, and F. Kurdahi, "Newertrack: Ml-based accurate tracking of in-mouth nutrient sensors position using spectrum-wide information," *IEEE Transactions on Computer-Aided Design of Integrated Circuits and Systems*, vol. 39, no. 11, pp. 3833–3841, 2020.

[29] N. Rashid and M. A. Al Faruque, "Energy-efficient real-time myocardial infarction detection on wearable devices," in *2020 42nd Annual International Conference of the IEEE Engineering in Medicine Biology Society (EMBC)*, 2020, pp. 4648–4651.

[30] M. Dautta and M. I. Hasan, "Underwater vehicle communication using electromagnetic fields in shallow seas," in *2017 International Conference on Electrical, Computer and Communication Engineering (ECCE)*. IEEE, 2017, pp. 38–43.

[31] M. Dautta, "Computation of electromagnetic field propagation characteristics of a dipole antenna submerged in sea-water," in *2016 International Conference on Wireless Communications, Signal Processing and Networking (WiSPNET)*. IEEE, 2016, pp. 28–32.

[32] S. A. Hamid, W. Ismail, C. Z. Zulkifli, and S. Abdullah, "Dual band rfid-based blood glucose monitoring system in wireless sensor network platform," *Wireless Personal Communications*, vol. 103, no. 3, pp. 2229–2244, 2018.

[33] S. M. Rajesh, "Integration of active rfid and wsn for real time low-cost data monitoring of patients in hospitals," in *2013 International Conference on Control, Automation, Robotics and Embedded Systems (CARE)*. IEEE, 2013, pp. 1–6.

[34] A. V. Quintero, F. Molina-Lopez, E. Smits, E. Danesh, J. van den Brand, K. Persaud, A. Oprea, N. Barsan, U. Weimar, N. De Rooij *et al.*, "Smart rfid label with a printed multisensor platform for environmental monitoring," *Flexible and Printed Electronics*, vol. 1, no. 2, p. 025003, 2016.

[35] G. Liu, L. Mao, L. Chen, and S. Xie, "Locatable-body temperature monitoring based on semi-active uhf rfid tags," *Sensors*, vol. 14, no. 4, pp. 5952–5966, 2014.

[36] E. Waffenschmidt and T. Staring, "Limitation of inductive power transfer for consumer applications," in *2009 13th European Conference on Power Electronics and Applications*. IEEE, 2009, pp. 1–10.

[37] S. Han, J. Kim, S. M. Won, Y. Ma, D. Kang, Z. Xie, K.-T. Lee, H. U. Chung, A. Banks, S. Min *et al.*, "Battery-free, wireless sensors for full-body pressure and temperature mapping," *Science translational medicine*, vol. 10, no. 435, 2018.

[38] R. Lin, H.-J. Kim, S. Achavananthadith, S. A. Kurt, S. C. Tan, H. Yao, B. C. Tee, J. K. Lee, and J. S. Ho, "Wireless battery-free body sensor networks using near-field-enabled clothing," *Nature communications*, vol. 11, no. 1, pp. 1–10, 2020.

[39] F. Wen and X. Huang, "Human exposure to electromagnetic fields from parallel wireless power transfer systems," *International journal of environmental research and public health*, vol. 14, no. 2, p. 157, 2017.

[40] P. K. Joseph, D. Elangovan, G. Arunkumar, and A. A. Zekry, "Overview of different wpt standards and a simple method to measure em radiation of an electric vehicle wireless charger," in *2019 IEEE MTT-S International Microwave and RF Conference (IMARC)*. IEEE, 2019, pp. 1–8.

[41] "nRF51 SDK: Gazell Link Layer User Guide." [Online]. Available: https://developer.nordicsemi.com/nRF5_SD

[42] A. B. Junaid, A. Konoiko, Y. Zweiri, M. N. Sahinkaya, and L. Seneviratne, "Autonomous Wireless Self-Charging for Multi-Rotor Unmanned Aerial Vehicles," *Energies*, vol. 10, no. 6, p. 803, Jun. 2017.

[43] X. Lu, D. Niyato, P. Wang, D. I. Kim, and Z. Han, "Wireless charger networking for mobile devices: fundamentals, standards, and applications," *IEEE Wireless Communications*, vol. 22, no. 2, pp. 126–135, Apr. 2015.

[44] H. Hwang, B. Lee, S. Park, C.-H. Jeong, C. Kwon, H. Kim, and S.-W. Kim, "Power transfer characteristics of four-coil magnetic resonance system according to the position of self-resonant coils," in *2013 USNC-URSI Radio Science Meeting (Joint with AP-S Symposium)*, Jul. 2013, pp. 117–117.

Manik Dautta is currently a Ph.D. student in Electrical Engineering at the University of California, Irvine (UCI). He received his bachelor's and master's degrees both in Electrical and Electronic Engineering from Bangladesh University of Engineering and Technology, Bangladesh. His research is mostly focused on recently emerged wearable, conformal, and body mounted sensors with special interest on the integration of biosensors into wearable and flexible RF sensor platforms.

Abel Jimenez is currently a Researcher in Biomedical sensors at the University of California, Irvine. His current research involves miniaturization of biomedical sensors and wireless power transfer. He graduated from UCI in 2019 and holds a diploma in Computer Engineering. He is starting his master's in Electrical Engineering at UCI in 2020. His current interests are embedded system development and machine learning.

Kazi Khurshidi Haque Dia is currently a Ph.D. student in Electrical Engineering at University of California, Irvine (UCI). She received her B.Sc. degree from Ahsanullah University of Science and Technology, Bangladesh and M.Sc. Degree from Bangladesh University of Engineering and Technology, Bangladesh both in Electrical and Electronic Engineering. Currently her Ph.D. research interests include flexible wearable devices and biosensors. She is a graduate student member of IEEE.

Nafiul Rashid is currently a Ph.D. student in Computer Engineering at the University of California, Irvine (UCI). He received his bachelor's and master's degree both in Computer Science and Engineering from Islamic University of Technology (IUT), Bangladesh. His research is focused on energy-efficient embedded systems and Cyber-Physical Systems (CPS) with a special interest in mobile healthcare, wearable devices, and edge machine learning. He is a graduate student member of the IEEE.

Mohammad Abdullah Al Faruque is currently an associate professor at the University of California, Irvine (UCI). He is directing the Embedded and Cyber-Physical Systems (AICPS) Lab. He received his Ph.D. degree in Computer Science from Karlsruhe Institute of Technology, Germany in 2009. His current research is focused on the system-level design of embedded and Cyber-Physical Systems (CPS) with a special interest in model-based design. He is the senior member of both the ACM and IEEE.

Peter Tseng is currently an assistant professor of Electrical Engineering and Computer Science at the University of California, Irvine (UCI). He received his bachelor's degree from the University of California, Berkeley, and his Ph.D. degree from the University of California, Los Angeles. His research interests include wearable devices, biosensors, and cellular microdevices. He combines the ideas from both the natural and engineered worlds to create systems that seamlessly connect to living bodies.

2327-4662 (c) 2020 IEEE. Personal use is permitted, but republication/redistribution requires IEEE permission. See http://www.ieee.org/publications_standards/publications/rights/index.html for more information.
Authorized licensed use limited to: Access paid by The UC Irvine Libraries. Downloaded on January 27,2021 at 01:00:16 UTC from IEEE Xplore. Restrictions apply.